

# Correcting for Non-Linearity in FOC Imaging Data

D. A. Baxter<sup>1</sup>

## Abstract

An extensive analysis has been performed to characterize the non-linear response of the FOC f/96 detector, particularly in the presence of point sources. We describe the analysis and discuss the rationale involved, and in conclusion present some empirical formulae which can be used to compensate for the effects of point source non-linearity in a sensible, but conservative, manner. We also examine and quantify two sensitivity effects which influence photometry; the format-dependent sensitivity variation, and the position-dependent effect induced by the FOC scanning beam.

## I. Introduction

Most forms of analysis applied to FOC imaging data are influenced to a greater or lesser degree by the fact that the detector response is non-linear. Quantitative analyses such as aperture photometry can be seriously compromised by point source non-linearity, and even qualitative cosmetic procedures can be affected. This report is the latest in a series of investigations of the effects of non-linearity in the FOC. The response of the detector to extended illumination, as with flatfields, has been investigated and quantified by Jedrzejewski and the results are described in the latest version of the FOC Handbook (Nota et al., 1993, hereafter Ref 1). A more recent investigation of the effects of point source non-linearity has been carried out by Greenfield (1993) and describes a solution which appears to work for the special case where the observed peak count rates are low. The method derives from a low count rate assumption which limits its applicability, and it also lacks generality in that the correction is applied, not to the image data, but to the aperture photometric data. Also, the sample of stars used for the analysis had to obey specific selection criteria regarding their position within the image and the local stellar density distribution. This implies a considerable selective, and subjective, preparation of the data before the non-linearity correction can be applied.

In this report we present a method which offers the possibility of a completely general correction which is applied directly to the image data without requiring any prior knowledge of the image contents. Although our method derives from the same basic precepts, regarding the detector operation, our approach to dealing with the problem is completely different. We begin with a discussion of what causes non-linearity and saturation in FOC images.

---

1. Space Telescope Science Institute, Baltimore, MD 21218

## Causes of Non-Linearity and Saturation

FOC non-linearity occurs because of the photon-counting nature of the detector. Incoming photons pass through the image intensifier tube of the FOC and finally manifest themselves as a photon event on the Target TV Tube. A detection aperture (approximately  $4 \times 9$  pixels), scans across the target surface and the locations of individual photon events are measured (by centroiding), and placed in the Science Data Store (SDS). A single photon event has a full width at half maximum of  $\sim 4$ - $5$  pixels. If two or more photon events overlap in the course of a single scan then, if the events are very close together (i.e. the area is not much greater than a single photon event) the detector will register one event, regardless of how many photons were involved. If the overlap is smaller, and the event is significantly larger than a single photon event then the Video Processing Unit (VPU) detection logic will classify it as an ion event and reject it, registering nothing. [The description of the VPU detection logic given here is simplified and is intended only to provide a basis for understanding the kinds of discrimination used by the logic, and how the application of this logic leads to non-linearity. For example, the logic can discriminate some types of overlapping event; however, we are only really concerned with cases where the logic is incapable of discriminating.]<sup>1</sup> In either case, the detector undercounts the number of incident photons. This is what we refer to as non-linearity.

The next point to consider is: when does non-linearity become saturation? Consider first the case of uniform illumination. Since the flux is spatially uniform and constant, we can describe the distribution of photon events within a single scan by using, for example, the average separation between neighboring events. This parameter will be approximately constant for any given flux and will decrease as the flux increases. In this case, overlapping events will occur more and more frequently. Also, since overlapping events are much larger than single photon events, they are classified as ion events and rejected, i.e. the VPU Detection Logic will register fewer and fewer events as the incident flux continues to rise. In the limit, it can be seen that eventually a point will be reached where every event is considered to be an ion event, and as a result, the scan would register nothing. So for uniform illumination, a plot of measured count rate against incident count rate would show a clear maximum followed by a fall-off to zero. By implication, for every measured count rate less than the maximum there are two possible values for the incident value, although for extended sources it is usually not difficult to decide where on the curve your data is located, (unless you are close to the maximum). Also, for extended sources it is relatively easy to define the saturation point since this is considered to be the point at which the measured count rate starts to fall.

For point sources the situation is slightly different since most of the photons are concentrated in a small area. In this situation the core of the PSF, which at half maximum is somewhat narrower than a single photon event ( $3 \times 3$  pixels), will register as a single photon so long as the count rates are relatively low. The PSF however, is not a true point source and so, as the flux increases, the area occupied by PSF core photon events within a single scan will increase and obviously, at some

1. The detailed descriptions of the VPU Detection Logic are given in the "Photon Detection Assembly (PDA) Handbook," issued by British Aerospace (Dec. 1979. Document Number SE-FD-B002).

point, will exceed the detection logics limit for the size of a single photon event. It will then be classified as an ion event, and rejected. At this point, the measured count rate in the core of the PSF will start to fall off, while the surrounding areas (receiving a lower flux) will continue to rise. Hence, for very bright point sources the image which is registered in the SDS will have a hole where the core should be, which is exactly what we see. There will be a maximum central count rate that can be measured in a point source, but this will be higher than for an extended source since most of the incident photons in the PSF core are superposed and will still register as a photon event; in addition, there are many fewer photons in the region surrounding the core and therefore relatively few overlapping events. Because of this, saturation does not occur for point sources until the PSF core event size per scan is significantly greater than a single photon event.

### The Approach

Ideally, we would like a procedure which can be applied indiscriminately to any and all FOC imaging data, and which will correct for non-linearity, on a pixel-by-pixel basis and irrespective of the image structure, in a manner which is both sensible and conservative. It should be clear from the preceding discussion however, that it is unlikely that we will ever be able to deal sensibly with pixels which are saturated, or for that matter, seriously non-linear. The analysis and solutions which are presented in this report are therefore, only applicable to data with low to moderate levels of non-linearity (i.e. less than 40-50 percent non-linear), defined by:

$$percent = \frac{Incident - Measured}{Incident} \times 100.$$

As we have noted, the level of non-linearity present in FOC images depends primarily on three factors:

- The rate at which the photons are arriving at the detector.
- The spatial distribution of the photons on the detector (i.e. the image structure).
- The frequency with which the detector is being scanned.

The time in seconds taken by the read beam to complete one scan of the detector is given by:

$$T_f = \frac{z(S \times L)}{8.8 \times 10^6} \tag{1}$$

(Ref 1), where the numerator ( $S \times L$ ) defines the area of the imaging format and  $z$  indicates the pixel type ( $z = 1$  for normal, and  $\approx 2$  for zoomed pixels). From (1) it can be clearly inferred that smaller formats can measure higher count rates since they are being scanned at a higher frequency. As mentioned above, the linearity

performance depends also on the structure within the image. Under uniform illumination photons arrive at a constant rate but are distributed over the detector, in which case the amount of non-linearity depends on the scan time and the separation between neighboring events. For illumination by a point source however, the non-linearity is dependent on the PSF core event size within a single scan, which determines whether the VPU detection logic registers a single photon event or nothing. Under uniform illumination there is a genuine and rigid maximum count rate that can be registered by the VPU, which for a  $512 \times 512$  image is  $\sim 6$  counts/pixel/sec (Ref 1, see Figures 28 & 29). However, since the peak flux from point sources is very localized, i.e. in an area much smaller than the scanning aperture and only slightly larger than the photon event size, this restriction does not apply, and peak count rates far in excess of this value can be recorded.

The factor which governs the way in which the VPU logic responds at any point in the scan, is clearly the photon/event distribution within the scanning aperture. Flux distributions or concentrations with characteristic widths smaller than the scanning aperture will cause a response similar to that seen for point sources, whereas, any flux distribution which does not vary by much across the aperture will produce the kind of response associated with uniform illumination. With this realization comes the first glimmer of hope for a solution; *vis.* if we can separate an image into its two components, i.e. an extended component and the 'point-like' component, then each can be dealt with separately.

The non-linear response to uniform illumination is relatively well understood, and can be modelled using a form originally suggested by Jenkins (1987),

$$r = a \left( 1 - \exp\left(\frac{-\rho}{a}\right) \right),$$

where  $r$  is the measured count rate,  $\rho$  is the true count rate and  $a$  is a fitting parameter. This model gives an excellent fit to the observed data for count rates up to 80 percent of the saturation level. Inverting this equation we get;

$$\rho = -a \ln\left(1 - \frac{r}{a}\right), \quad (2)$$

which should reliably correct the observed count rates of the extended component of an image (again, up to  $\sim 80$  percent of saturation). All that then remains is to determine a suitable correction for the second component containing all the point-like features. Finally, the fully corrected image would be obtained by recombining the corrected versions of the two separate components.

## II. Analysis

We have shown that the FOC detectors respond differently to extended and point source illumination. We have also specified that the definitions of these types of illumination are related to the scanning aperture size in that the detector point source response applies when the aperture encounters structures which vary by large

amounts in intensity over short scale lengths of only a few (4-5) pixels, everything else in the image qualifies as extended. In order to proceed with the analysis therefore we must separate our image into these two components.

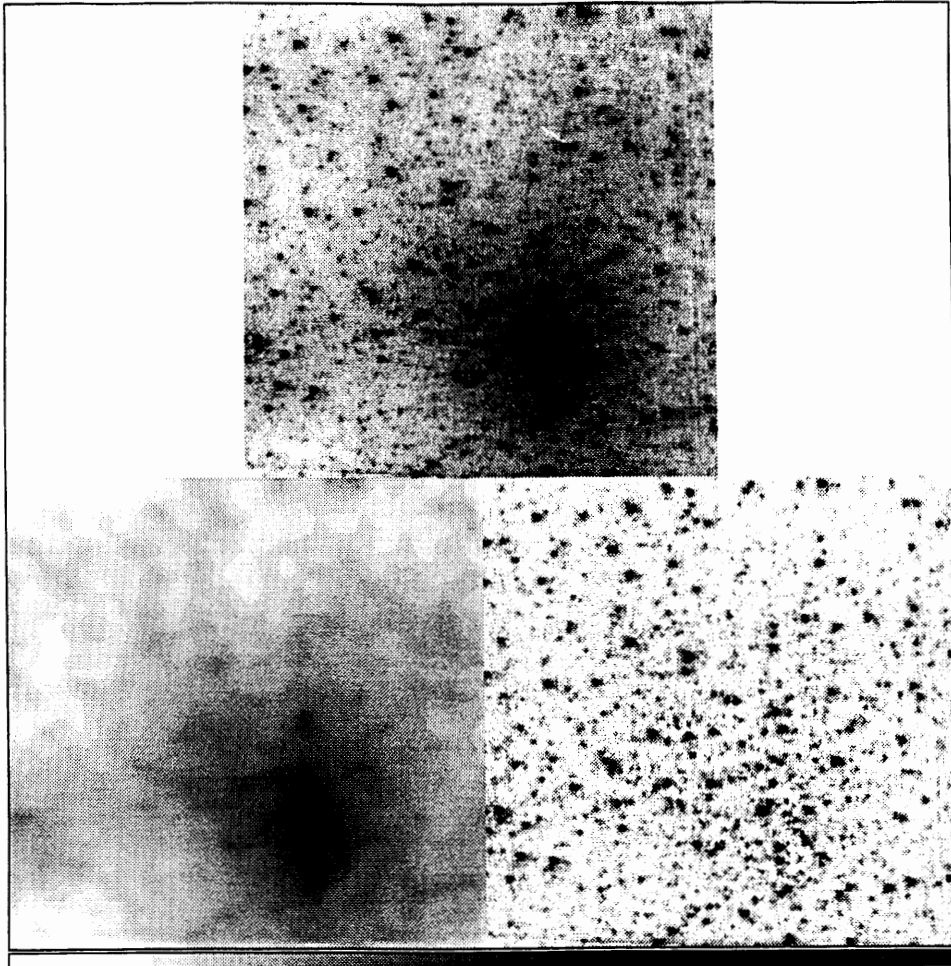


Figure 1: Background determination and removal. At the top is the  $512 \times 512$  (normal), F2ND image. The bottom left shows the Background obtained by application of the median filter. At the bottom right is the difference image containing only the point-like structures, i.e. the PSF cores.

For the purposes of this analysis we use a series of observations of the core of M15 (NGC7078), which were obtained on 14th May 1992 as part of the Cycle 2 FOC Calibration Plan. In particular we concentrate on two images, both in the  $512 \times 512$  (NORMAL) format. The first image was observed through the F342W+F2ND (2ND image) and the second through F342W+F2ND+F1ND, (3ND image).

### **Determine and Remove the Background Component**

The Background component of each image is estimated by application of an unweighted median filter. The size of the filter ( $9 \times 9$  box) is determined by the requirement that it should ignore all structures on scale lengths shorter than  $\sim 5$  pixels (see Figure 1).

### Correct for the Extended Component of the Non-Linearity

If we take two images,  $A$  and  $B$  (say), of the same object and plot the pixel values  $A(i,j)$  against  $B(i,j)$ , then if the detector was perfectly linear the result would be a straight line graph where the slope would represent a simple scaling factor between the two images. When we carry out this procedure on FOC data the result, because of detector non-linearity, is not a straight line (see Figure 2). If a linear fit is carried out using only the pixels with low values (i.e. low count rates) then the deviation of the data from this fit indicates the level of non-linearity. After applying the extended component non-linearity correction, (Eqn 2), to both images, we see that the result is an almost perfect straight line distribution. This provides excellent support for the validity of this equation.

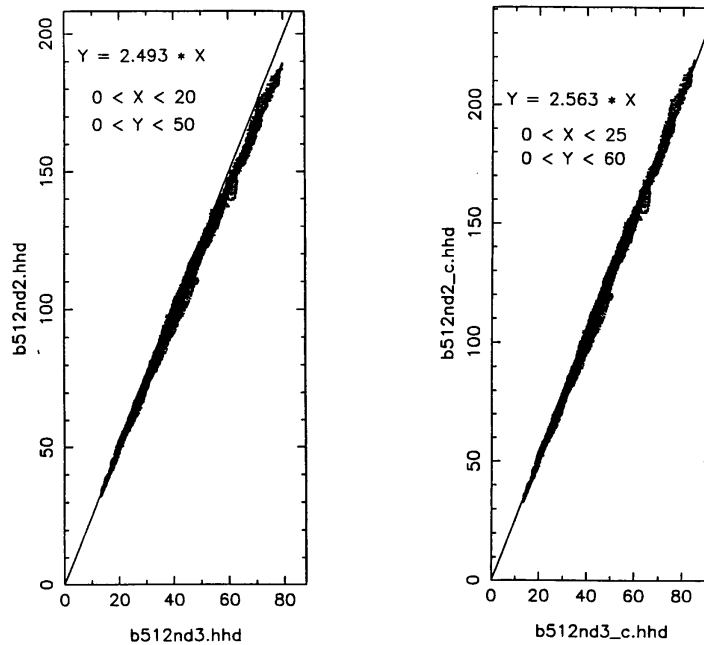


Figure 2: Comparison of background linearity before (left) and after (right) correction. Here we plot the pixel values from the two  $512 \times 512$  (normal) images against each other. The two images differ from each other only in that on (y-axis), has one less neutral density filter in the light path. It is clear that after application of the non-linearity correction, the low count rate fit extrapolates through the full range of measured count rates.

We apply the background correction to the data as follows. If  $B_{i,j}$  is the pixel value and  $\beta_{i,j}$  the count rate at position  $(i,j)$  in the extracted background image, then the corrected, 'linear' count rate,  $\beta'_{i,j}$  is given by;

$$\beta'_{i,j} = -a \ln\left(1 - \frac{\beta_{i,j}}{a}\right),$$

where  $a$  is the linearity parameter referred to earlier, and the corrected pixel value,  $B'_{i,j}$  is then;

$$B'_{i,j} = B_{i,j} \frac{\beta'_{i,j}}{\beta_{i,j}}.$$

Since the background non-linearity will affect how the detector responds to an overlying point source, this correction must also be applied to the point source component. This is equivalent to the observation that the response of the detector to a point source with a given peak count rate will vary according to the background count, or in the case of this data, with the stellar density and brightness distribution in its immediate neighborhood, i.e. a star in the cluster centre will be more non-linear than a similar star in a more sparsely populated region. Hence we also have;

$$S'_{i,j} = S_{i,j} \frac{\beta'_{i,j}}{\beta_{i,j}},$$

where  $S_{i,j}$  refers to the background-subtracted, point-source image, and  $S'_{i,j}$  is the point source image corrected for the non-linear effects of the background.

When all of these procedures have been carried out, for all of the extracted sub-images, we are then in a position to proceed with determining the point source non-linearity correction.

### Correcting the Point Source Component

Before we can proceed with this part of the analysis, it is necessary to define a reference image, i.e. an image which is assumed at the outset to be fairly linear. For this purpose we use the 3ND image which is theoretically more linear than the 2ND image by a factor of  $\sim 2.5$  (Note: this is only an initial assumption and the non-linearity of the reference is re-addressed later).

The next step is to select a sample of stars which are going to be used to compare the fluxes between the images. For this purpose we initially selected all of the stars within the reference image with a peak count greater than 50, which gave an initial sample of 135 stars. We then rejected any stars which were influenced by obvious blemishes and reseau marks (42 stars rejected). Finally we rejected any stars which showed evidence of being intrinsically variable. This removed a further 30 stars, mostly faint, and left a sample of 63 stars with peak count rates between 0.04 and 1.1 counts/pixel/sec in the reference image.

In Figure 2 we empirically determined the scaling factor between these two images, i.e. for the F1ND filter, as being 2.563 so in order to directly equate them, we first scale the reference by 0.974, to adjust for the exposure difference, and then multiply by 2.563, to correct for the neutral density filter. After these adjustments, the comparison image should give a one-to-one correspondence with the reference, except for the effects of image non-linearity.

We next use a  $5 \times 5$  pixel aperture to determine the peak count rate and the total aperture count for each star in our comparison sample. This is done for both images

and the ratios;

$$R(\text{peak}) = \frac{\text{Observed Peak Count Rate}}{\text{Reference Peak Count Rate}}$$

and

$$R(\text{ap}) = \frac{\text{Observed Total Count}}{\text{Reference Total Count}}$$

are calculated, and plotted against the *observed* peak count rate (see Figure 3). It can be seen that the variation of the ratios is much the same for both count rates and total counts. However, the scatter in the data is much greater in the count rate ratio,  $R(\text{peak})$ , as you would expect.

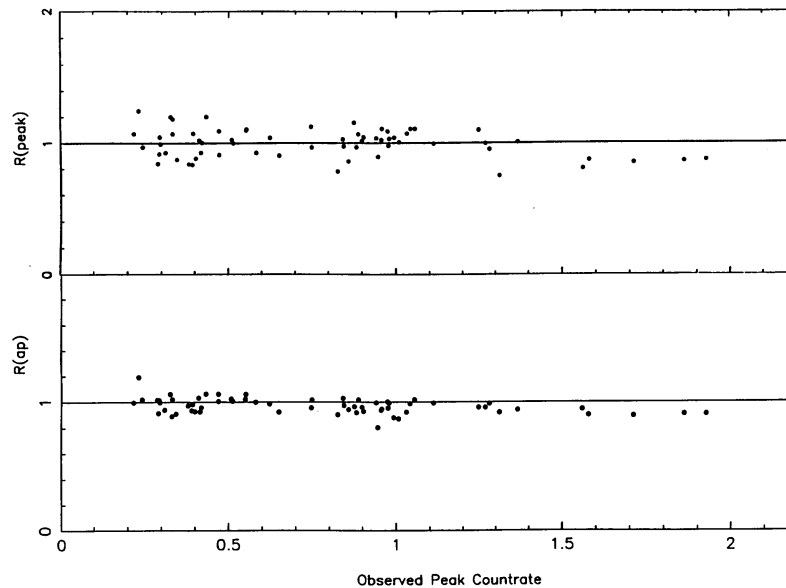


Figure 3: The non-linearity of the point source images in the  $512 \times 512$  format, as indicated by the peak count rates (top), and the total aperture counts (bottom), for our sample of 63 comparison stars.

To provide an empirical correction for levels of non-linearity demonstrated in Figure 3 we require only the fitting of some analytic form to the observed ratio distribution. We start with  $R(\text{peak}) = f(r)$ , where  $f(r)$  is some function of the observed count rate,  $r$ . Then if the true peak count rate,  $\rho$ , can be equated to the reference peak count rate,  $\rho'$  (say) we can write:

$$R(\text{ap}) \approx R(\text{peak}) = \frac{r}{\rho'} \approx \frac{r}{\rho} = f(r),$$

and therefore the 'true' count rate can be expressed as;

$$\rho \cong \frac{r}{f(r)}. \quad (3)$$

Examining the data in Figure 3, it is clear that a 'straight-line' model would adequately fit the data, however since the amounts of non-linearity measured are relatively small, (only about 10 percent), this may be over simplistic. For the point sources which have peak count rates less than  $\sim 0.6-0.7$  counts/pixel/sec there is no significant deviation from linear (at least with respect to the aperture ratios, and so a simple correction of this type would over-correct in these regions. This being the case, we have made the next simplest assumption, i.e. that the relationship is quadratic and that,

$$f(r) = A + Br + Cr^2,$$

implying that  $A = 1$ , (since  $R(\text{peak}) = R(\text{ap}) = 1$ , for small  $r$ ). Carrying out a least-squares quadratic fit to these data we obtain that  $B = -0.013 \pm 0.003$  and  $C = -0.017 \pm 0.003$ .

We now return to consideration of the 'reference' image. As we mentioned earlier, the linearity of the reference image is clearly not guaranteed and so we took this result only as a first solution. The main application of this first determination of  $f(r)$  was to apply a correction to the reference data. Although it cannot be shown that this would make the reference perfectly linear, it should be a reasonable assumption that this correction would improve its linearity. Having said that, it will be demonstrated that the application of this correction had very little effect on the subsequent analysis since the linearity of the reference was already pretty good and the correction only significantly affected the small number of bright point sources.

Using the modified reference data, we then repeated the analysis of this format as far as the determination of the coefficients of  $f(r)$  and obtained the result that  $B = -0.014 \pm 0.002$  and  $C = -0.017 \pm 0.003$ . Since the coefficients were so similar we combined these to obtain;

$$f(r) = 1 - \alpha(r + r^2), \quad (4)$$

where  $\alpha = 0.016 \pm 0.003$ .

Now that we have the model defined, we can examine the limitations pertaining to its application. It is a trivial exercise to determine that the model has a positive maximum, i.e. predicts a maximum measurable count rate, at  $r \approx 2.75$  counts/pixel/sec (see Figure 4), which equates to a 'true' count rate of  $\rho = 4.3$  counts/pixel/sec. This would represent 57 percent non-linearity (as defined in Section I). Obviously, since we are extrapolating beyond our data set, we do not claim that this represents the true saturation point, however it does define the maximum correction which can be applied using this model. The model can also, of course be refined when better data are obtained (in Cycle 4). As a final check, we corrected the data pixel by pixel, (using Eqn 4), and then re-ran the analysis using a complete series of apertures with radii from 2-9 pixels. From this we concluded that there is no significant aperture dependence imposed by this procedure.

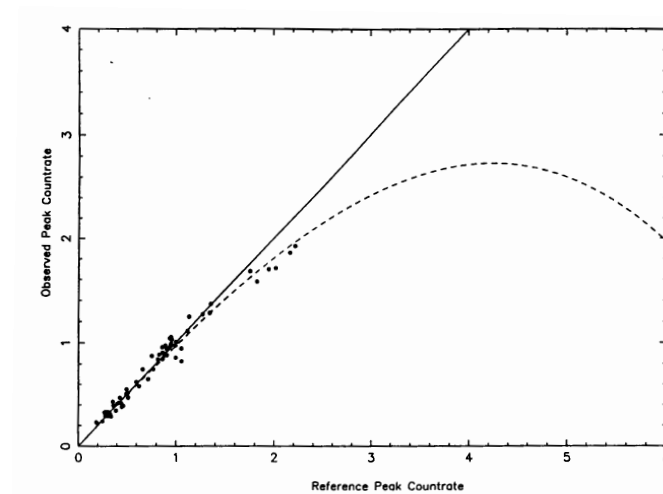


Figure 4: Comparison of the proposed model with the observed data.

### Format Dependent Response Variation

The appropriate subsection of the extended source component of the  $512 \times 512$  (zoom) format was corrected for extended source non-linearity and then compared to the reference image by plotting the growth curve (c.f. Figure 2.). The result was a nice straight line, but with a slope of 1.44, i.e. this zoomed format is 44 percent more sensitive to extended emission than the normal format. The existence of this format dependence was previously known and the magnitude of the sensitivity difference derived here is consistent with that derived by Greenfield (1993), *vis.* 40 percent, however the cause is not clear.

We then repeated the same comparison using the  $512 \times 1024$ (zoom) format and after appropriate scaling, to allow for exposure time and 1ND difference in filters, we determined that for this format there was a 29 percent increase in the extended source sensitivity compared to the reference, which again is consistent with the value determined by Greenfield (1993) of 25 percent.

Our next step was to scale these images by the above factors, (to make the background responses the same for all formats), and then the ratios,  $R(peak)$  and  $R(ap)$ , were determined. It should be noted that the highest observed peak count rate measured in the  $512 \times 512$  format was only  $\sim 6$  counts/pixel/sec, and only  $\sim 0.3$  c/p/s in the full format. When the data were plotted (Figure 5), there was no evidence for non-linearity in either data set (almost certainly because of the low count rates). The only obvious indication is of a scale or response difference, in that the aperture fluxes in the zoomed data are only 90 percent of the normal data.

An examination of the effect of zoom/dezoom on the peak count rate in zoom format data does indicate that a drop of 10 percent can occur, (depending on the position of the point source centroid within the brightest pixel), however this should not occur with the aperture fluxes since the problem can be overcome by simply increasing the aperture size. To test this we doubled the aperture size (to  $9 \times 9$  pixels) and recalculated. The result still showed that the zoomed data was only 91 percent of the reference. Clearly, if increasing the aperture is the required solution, the

required aperture size would be unusably large. The bottom line to this result appears to be that whatever causes the format dependent sensitivity difference produces a different response for extended sources and point sources.

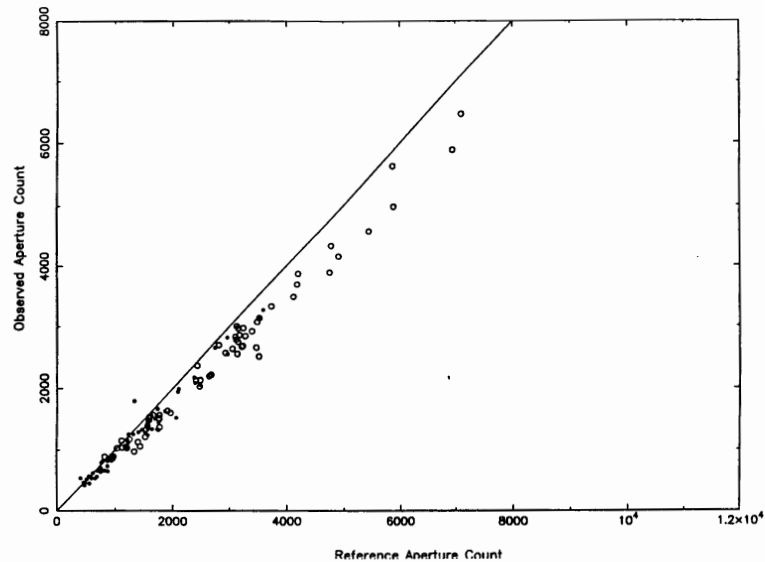


Figure 5: Aperture data for the zoomed formats compared to the reference,  $512 \times 512$  (zoomed) (open circles), and  $512 \times 1024$  (zoomed) (filled circles). The zoomed point source response is only  $\sim 90$  percent of that seen for normal pixel data.

### III. Discussion

#### Point Source Non-Linearity

We have determined that, at least for the  $512 \times 512$  (normal) format, a reasonable and conservative correction for point source and extended source non-linearity is possible. Both corrections are necessary because, spherical aberration places an extended component around every point source, and since the extended component saturates at a much lower count rate than the PSF core component itself, it is likely that the extended halo non-linearity accounts for the major part of the total PSF non-linearity.

Because of the low count rates present in the zoomed formats, we have been unable to determine a non-linearity correction for these formats.

#### Format Dependence

Comparisons of data obtained in different formats show that, after correction for non-linearity, the extended component of the  $512 \times 512$  (zoomed) format is 44 percent ( $\pm 4$  percent) more sensitive than the reference image, i.e. the  $512 \times 512$  (normal) format. Similarly, the  $512 \times 1024$  format is 29 percent ( $\pm 3$  percent) more sensitive than the reference. However, an anomaly appears when we compare the point source data. After correcting for the sensitivity difference, we find that the zoomed pixel formats are only  $\sim 90$  percent as responsive to point sources as is the reference normal pixel format.

It is not at all clear why this should be the case, however, it almost certainly indicates some fundamental difference in the operation of the Photon Detection Logic when operating in zoom mode.

### **References**

- Nota, A., Jedrzejewski, R.I., Hack, W., (1993), *Faint Object Camera Instrument Handbook [Post-COSTAR], Version 4*  
Greenfield, P., (1993), *FOC Instrument Science Report - FOC-074*  
Jenkins, (1987), MNRAS, 226, 341.